Atmospheric Patterns over the Antarctic Peninsula

SERGI GONZALEZ

Antarctic Group, Spanish Meteorological Service (AEMET), and Department of Applied Physics, University of Barcelona, Barcelona, Spain

FRANCISCO VASALLO

Antarctic Group, Spanish Meteorological Service (AEMET), Rota, Spain

CAYETANA RECIO-BLITZ

Departmento de Matemática Aplicada a las Tecnologías de la Información y las Comunicaciones, Universidad Politécnica de Madrid, Madrid, Spain

JOSÉ A. GUIJARRO

Balearic Islands Office, Spanish Meteorological Service (AEMET), Palma, Spain

JESÚS RIESCO

Antarctic Group, Spanish Meteorological Service (AEMET), Málaga, Spain

(Manuscript received 8 September 2017, in final form 8 January 2018)

ABSTRACT

Using clustering analysis for the sea level pressure field of the ERA-Interim reanalysis between 1979 and 2016, five synoptic pressure patterns have been obtained for the Drake area and Antarctic Peninsula (AP) region (45°–75°S, 20°–120°W), and the resulting daily series has been made available to the scientific community. The five patterns have been named according to their most important features as follows: low over the Weddell Sea (LWS), low over the Amundsen and Bellingshausen Seas (LAB), low over the Drake Passage (LDP), zonal flow over the Drake Passage (ZDP), and ridge over the Antarctic Peninsula (RAP). Each atmospheric pattern is described after analyzing its development and evolution. A frequency analysis shows that the five atmospheric patterns present a similar annual frequency but a large seasonal variability. The transitions from one pattern to another tend to follow a cycle in which synoptic atmospheric waves are displaced eastward by a quarter wavelength. Four of the five atmospheric patterns (all except RAP) are very influenced by the southern annular mode (SAM); however, only LAB and LWS are influenced to some degree by ENSO. The occurrence of the LAB pattern presents a positive trend showing agreement with other studies that indicate an enhancement of the Amundsen–Bellingshausen Seas low. Finally, atmospheric circulation patterns have been related to the airmass advection and precipitation in Livingston Island, showing the potential application for studying the changes in the surface mass balance on the AP cryosphere.

1. Introduction

Ice mass lost by mountain glaciers and island ice caps is one of the major contributors to sea level rise (IPCC 2013). Compared to those of large ice sheets, the thermal and dynamic responses of these ice masses are quicker, so they are more vulnerable to global warming. Most ice caps are located on islands around the Antarctic Peninsula (AP) (Bliss et al. 2013), and many studies have shown evidence of their acceleration and thinning (i.e., Hock et al. 2009; Radić and Hock 2010, 2011; Gardner et al. 2013).

Ice cap thinning occurs as a response to the changing conditions in the AP region. The AP has warmed +3.7°C century^{-1} during the second half of twentieth century (Vaughan et al. 2003), and although there has been a

Corresponding author: S. Gonzalez, sgonzalezh@aemet.es

DOI: 10.1175/JCLI-D-17-0598.1

significant cooling between 1998 and 2015 (Carrasco 2013; Oliva et al. 2017), Turner et al. (2016) demonstrated that this period is consistent with the natural variability of the region, since it is affected by long-term persistence (Ludescher et al. 2016). Indeed, the AP region is characterized by a large interannual variability, and its temperature is very sensitive to the state of both El Niño–Southern Oscillation (ENSO) (Fogt and Bromwich 2006; Fogt et al. 2011; Clem and Fogt 2013) and the southern annular mode (SAM) (Thompson and Solomon 2002; van den Broeke and van Lipzig 2003; Marshall 2003). It has been shown that these climatological modes of variability modify the main climatic patterns in Antarctica [i.e., the Amundsen–Bellingshausen Seas low (ABSL), jet streams], suggesting that their change may be closely linked to synoptic pressure patterns (Carleton 2003; Pezza et al. 2012).

Synoptic-scale systems eventually determine the temperature and moisture of the air mass that contribute to the surface mass balance of the ice caps in the AP. Therefore, a further understanding of the synoptic climatology and its relationship with other climatological parameters may help us interpret the changes in the AP cryosphere.

Although the AP climatology has been extensively studied, only a few studies have addressed the synoptic climatology and its classification. Kejna (1993) used a low-level analysis in the AP region between 1986 and 1989 to make a classification according to the airmass advection at H. Arctowski Station on King George Island. Govorukha and Timofeyev (2002) made a visual analysis with a set of synoptic charts, satellite imagery, and other operational information during three years between 1997 and 2000 to describe the main synoptic processes over the AP. Turner et al. (1998) examined satellite imagery and operational data to analyze synoptic-scale low pressure systems in the AP region during a year, classifying them according to the environment in which the cyclogenesis took place. Finally, Turner et al. (1996) used a comprehensive dataset, including observational data, satellite imagery, and numerical analyses and forecasts, during two special observation periods in 1994 and 1995, to produce high-quality analyses and assess the quality of the data at that time, although they did not address the classification of the synoptic data.

These studies have contributed to improving the knowledge of the synoptic activity in the AP region, but until now, no one has conducted an objective synoptic classification during an extended period of time and using clustering techniques. The use of clusters allows us to classify the synoptic atmospheric patterns without a high level of abstraction and is a practical and intuitive methodology for both meteorological sciences, including weather forecasting, and other sciences that require linking their findings with the weather in the region. To fill this gap, this classification is addressed in this paper. Datasets and the methodology used are detailed in section 2. In section 3 the synoptic classification is described, with an analysis of the trends and the relationship between the synoptic patterns found and different modes of variability. In section 4 we conduct an analysis comparing the synoptic patterns with the air mass advected over Livingston Island, discussing the possible effects on the surface mass balance on the island glaciers. In section 5 we draw some conclusions. Recently, Cohen et al. (2013) developed an objective synoptic classification for the Ross Sea region using the NCEP reanalysis. This study may be considered as its natural extension to the AP region.

2. Datasets and methodology

a. *Cluster analysis*

To obtain the synoptic pressure patterns in the Drake area, we selected the mean sea level pressure (SLP) field of the ERA-Interim reanalysis (Dee et al. 2011) using the native horizontal resolution (~80 km) interpolated to a regular grid of 0.75°. ERA-Interim has been stated as being one of the most realistic reanalysis products to describe the SLP and geopotential height at 500 hPa in the Antarctic region (Bracegirdle and Marshall 2012). The area selected was 45°–75°S, 20°–120°W (Fig. 1a) and is wide enough to represent the climate patterns in the surroundings of the Drake area and the AP. This area may include a few points located at high altitudes in the Andean Mountains (South America) and Eternity Range (Antarctic Peninsula) that are not expected to affect the cluster analysis. By contrast, we carefully selected the area not to cover the Antarctic Plateau, an area with widespread high altitudes where SLP reduction is not valid. The period analyzed ranges from 1 January 1979 until 31 December 2016. As synoptic features have a typical time scale from one to a few days, we do not expect significant changes in patterns in less than one day. So, for each day, we only employed the 1200 UTC field as the SLP field that better represents the synoptic pattern of that day, which will be compared with mean daily values from the automatic weather station (AWS) [see section 2c].

The approach we used for clustering was similar to that used by Cohen et al. (2013). Prior to clustering, we detrended the data by removing the mean SLP and weighted each data point by the square root of the cosine of the latitude. Thereafter, we retrieved the atmospheric

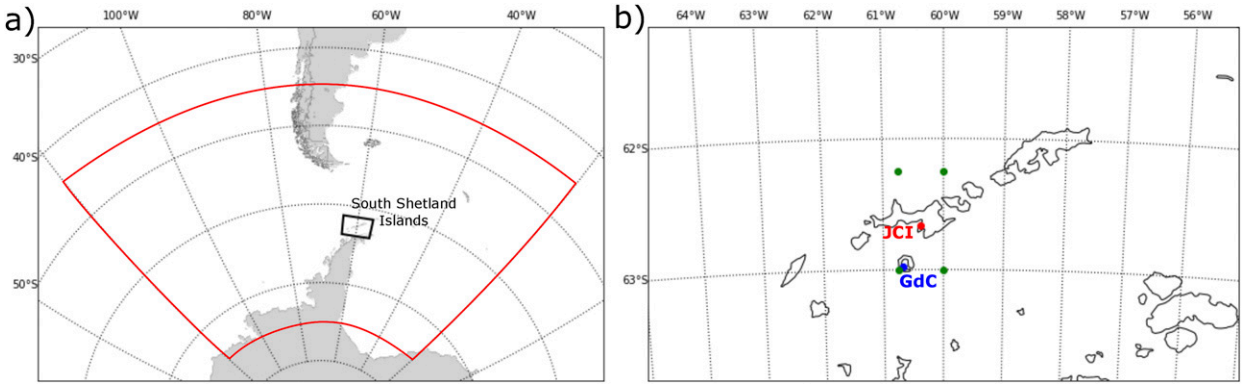

FIG. 1. (a) Map of the geographic area showing the area used to perform the cluster analysis (red) and the area depicted in (b) (black). (b) South Shetland Islands region indicating the JCI station (red), the GdC station (blue), and the four ERA-Interim reanalysis points used to homogenize the data (green).

patterns using the *k*-means cluster algorithm because of its proven performance in the synoptic meteorology in other regions (e.g., Kidson 2000; Lana et al. 2007; Houssos et al. 2008; Cohen et al. 2013). This algorithm consists of minimizing the average squared distance between all points in the same cluster to identify the centers of the cells. The single *k*-means algorithm is very sensitive to the initial values and may give unsatisfactory solutions by achieving local minimums. Thus, we improved the seeding algorithm by employing the *k*-means++ method (Arthur and Vassilvitskii 2007) to guarantee to find optimal solutions. This methodology was performed for *k* number of seed patterns from 3 to 15 and was repeated 10 times for each *k* to ensure reproducibility (with this methodology the 10 cluster fields obtained for each *k* were almost identical). As in Cohen et al. (2013), the final *k* set was selected by visual inspection of the center fields according to the expertise of the Antarctic forecasters of the Spanish Meteorological Service (AEMET) that operates in the area, selecting K5 as the one that best reproduced the synoptic patterns of the AP area. The same procedure was also employed with the 500-hPa geopotential height fields obtaining a similar set of clusters for K5 and therefore is not considered hereinafter. The resulting daily series have been made publicly available through the AEMET repository (online at http://hdl.handle.net/20.500.11765/7914).

b. Climate indices

To evaluate the climatological variability of the synoptic patterns retrieved, the patterns were compared with the two main climate modes of variability linked to the AP climate: the southern annular mode and El Niño–Southern Oscillation.

SAM is the principal mode of variability of the Southern Hemisphere circulation, and its changes have a large impact on the AP climate (Marshall et al. 2006). Surface temperatures over the AP have been linked to the strengthening or weakening of circumpolar westerlies associated with the SAM (Thompson and Solomon 2002; van den Broeke and van Lipzig 2003; Marshall et al. 2006). The monthly station-based SAM index calculated by Marshall (2003) (available online at https://legacy.bas.ac.uk/met/gjma/sam.html) was used. This index is based on the zonal pressure difference between 40° and 65°S calculated using 12 stations, and it extends back until 1957.

Variability in the AP temperatures has been also associated with the phase of ENSO by modulating the depth and the extension of the ABSL. We selected the El Niño–3.4 index calculated from the HadlSST1 dataset (Rayner et al. 2003) (available online at https://www.esrl.noaa.gov/psd/gcos_wgsp/Timeseries/Nino34/) as an index representative of the ENSO state (Bamston et al. 1997).

c. Station-based data

In section 4, we compare the synoptic patterns with the distribution of daily mean temperature, relative humidity, and accumulated precipitation observed to study the air masses advected over the AP. Data from the Spanish Base Juan Carlos I AWS (JCI; 62.66°S, 60.39°W) (Bañon and Vasallo 2015) on Livingston Island (South Shetland Islands) have been used to analyze the air mass advected to the South Shetland Islands for each synoptic type (Fig. 1b). A dataset of mean daily values of temperature, relative humidity, and precipitation accumulated from 2005 to 2016 was obtained if at least 80% of the daily 10-min values were available. To standardize the observations and fill the gaps, the dataset has been homogenized against the daily values at another AWS located at Gabriel de Castilla Station

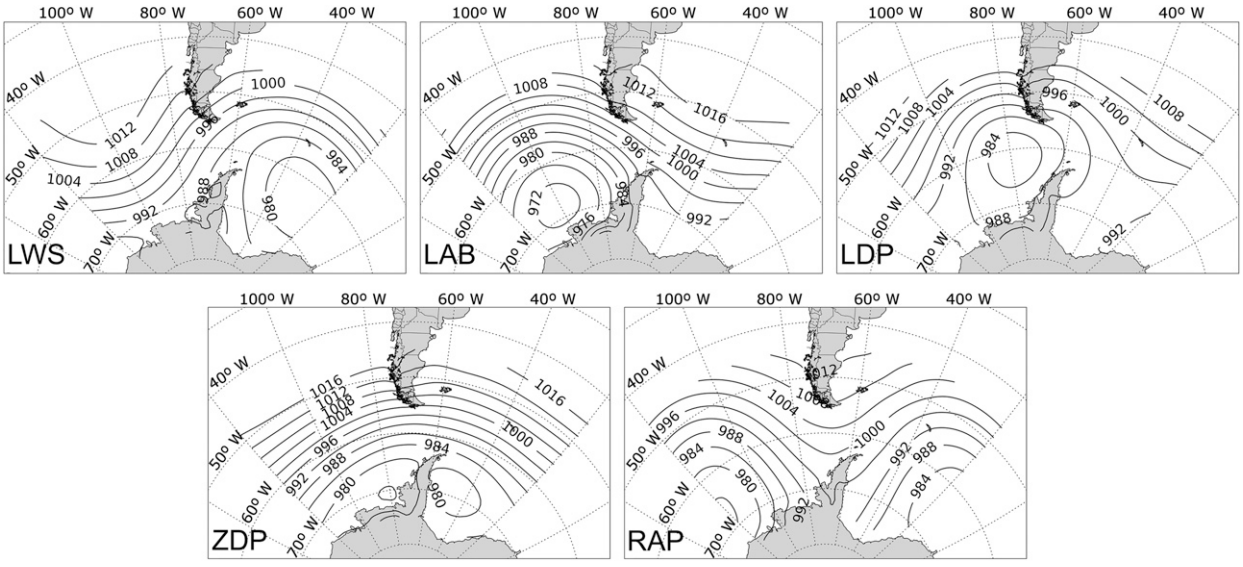

FIG. 2. Synoptic patterns (cluster centroids) calculated using ERA-Interim reanalysis data for the AP region over the period between 1979 and 2016.

(GdC; 62.98°S, 60.68°W) on Deception Island and the surrounding grid points of the ERA-Interim reanalysis (four points located at the intersections between 62.25°S, 60.75°W, 63.00°S, and 60.00°W) (Fig. 1b). The homogenization was performed by means of the R package Climatol (Guijarro 2017), applied on the monthly aggregates to improve the break point detection. Two significant break points were detected in the JCI temperature series and three in GdC. The dates of the break points were refined with the aid of the metadata of the stations before adjusting their daily series. The same procedure was applied to the relative humidity (one break point in JCI and two in GdC) and precipitation (one break point in JCI) series. Finally, the monthly means were subtracted from the daily means to obtain daily anomalies to compare them with the atmospheric patterns retrieved.

3. Synoptic patterns in the Antarctic Peninsula

a. Description of synoptic patterns

Figure 2 shows the five SLP synoptic patterns (the centroid of each cluster) calculated between 1979 and 2016 from ERA-Interim data. Besides evaluating the centroids, we also analyzed each pattern by examining some individual days (about 10 for each one) using Integrated Data Viewer (UCAR/Unidata) software. Figure 3 presents some examples of the synoptic maps and their classification. For clarity, each cluster has been named according to the most important feature; they are presented below.

1) LOW OVER THE WEDDELL SEA (LWS)

This cluster shows the presence of a low east of the Weddell Sea, produced either from the maxima of cyclogenesis located in the southern part of the Weddell Sea (Simmonds and Keay 2000; Simmonds et al. 2003) or from a low crossing the Drake Passage to the east. As a counterpoint, there is a presence of the South Pacific subtropical anticyclone extending to the southeast to the Bellingshausen Sea, sometimes even coupling with the continental Antarctic anticyclone. This pattern presents an intense meridional circulation from the south or southwest over the Antarctic Peninsula.

2) LOW OVER THE AMUNDSEN AND BELLINGSHAUSEN SEAS (LAB)

This cluster is characterized by the semipermanent ABSL located around 100°W at the easternmost climatological extension (Turner et al. 2013; Hosking et al. 2013; Raphael et al. 2016). This pattern is composed of wide quasi-stationary lows often surrounded by one or more small mobile lows. East of the Drake Passage, the South Atlantic subtropical anticyclone extends southward to the Weddell Sea, making this pattern almost symmetric with LWS. This cluster transports warm and moist air over the Antarctic Peninsula often associated with precipitation in the area (van Loon 1967).

3) LOW OVER THE DRAKE PASSAGE (LDP)

This cluster aggregates the lows over and west to the Drake Passage. These lows may have a zonal path crossing the Drake Passage to the east or a meridional

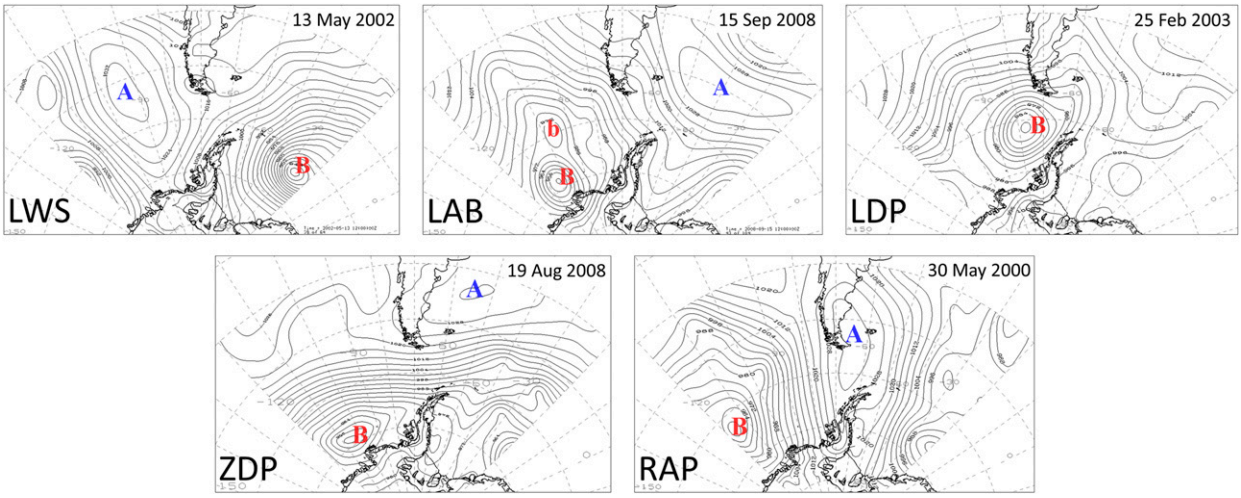

FIG. 3. Examples of ERA-Interim synoptic analysis in the AP for each cluster. LWS: 13 May 2002; LAB: 15 Sep 2008; LDP: 25 Feb 2003; ZDP: 19 Aug 2008; and RAP: 30 May 2000.

path either northward or southward as a result of a blocking high. Blocking highs are suggested in the cluster center by a slight ridge located over South Atlantic that sometimes couples with the Antarctic continental anticyclone.

4) ZONAL FLOW OVER THE DRAKE PASSAGE (ZDP)

This cluster is characterized by an intense westerly flow over the Drake Passage and Tierra del Fuego with mobile cyclones moving eastward at high latitudes along the circumpolar trough. Those cyclones cross from the Bellingshausen Sea to the Weddell Sea through the AP and may suffer a variety of orographic impacts on their paths (Mayes 1985).

5) RIDGE OVER THE ANTARCTIC PENINSULA (RAP)

This cluster presents a meridional circulation characterized by an anticyclonic ridge extending southward from South America to the Drake Passage and the AP associated with the wavenumber-3 pattern in the region (van Loon and Jenne 1972; Irving and Simmonds 2015). This ridge is flanked by two quasi-stationary wide lows, which enhance the meridional circulation. The western low may be associated with a western displacement of the ABSL.

b. *Frequency of occurrence*

The five atmospheric patterns each present a similar frequency all ranging between 18% and 22% (Table 1). The most common pattern is ZDP with a frequency of 22.0% of days, and the least common is LWS with 18.4% of days. There is a notable variability in pattern frequencies between seasons. For example, LAB shows an increase in frequency during the equinoxes, especially in the spring, associated with the semi-annual oscillation (SAO) when the wavenumber-3 pattern of the circumpolar trough (one of the troughs located over the Amundsen–Bellingshausen Seas) contracts and deepens southeastward (van Loon 1967; van den Broeke 1998, 2000; Simmonds and King 2004). The ZDP pattern also presents a noteworthy frequency in spring when the circumpolar trough contracts and enhances the zonal winds around Antarctica (Raphael 2004). In summer, when the polar jet moves slightly northward, the LDP pattern becomes dominant. It is possible that the classification method associates systems north of the ABSL inside the LDP pattern. This would explain the low occurrence of LAB in summer and the shift to the west of the LDP pattern in Fig. 1. Autumn and winter present a more equilibrated distribution of patterns, with a slight increase of RAP in both seasons and LWS in winter. The enhanced meridional circulation associated with those patterns may be linked with the winter intensification of the planetary wave activity (Raphael 2004; Hobbs and Raphael 2010; Irving and Simmonds 2015), the larger density of cyclones near the Flichner-Ronne ice shelf (Simmonds and Keay 2000), and a most western position of the ABSL (Hosking et al. 2013).

TABLE 1. Seasonal and annual frequency (%) of each synoptic pattern during the period between 1979 and 2016.

	LWS	LAB	LDP	ZDP	RAP
DJF	16.5	16.0	28.9	21.4	17.1
MAM	17.4	20.6	20.8	19.4	21.8
JJA	23.0	19.3	17.5	19.5	20.6
SON	16.5	26.0	13.7	27.8	15.9
Total	18.4	20.5	20.2	22.0	18.9

TABLE 2. Frequency (%) of pattern sequences between two consecutive days during the period between 1979 and 2016. Values in the diagonal (in bold) show the daily persistence for each synoptic pattern. Values in square brackets show the mean consecutive days in which each pattern persists. Values in parentheses show the frequency considering only the changing sequences, that is, when persistence is removed.

		To pattern				
		LWS	LAB	LDP	ZDP	RAP
From pattern	LWS	**12.6 [3.2]**	0.0 (0.0)	0.9 (2.5)	1.8 (5.1)	3.1 (8.8)
	LAB	0.0 (0.0)	**13.8 [3.1]**	2.7 (7.6)	3.1 (8.8)	0.9 (2.5)
	LDP	2.6 (7.4)	1.0 (2.8)	**12.9 [2.8]**	2.0 (5.7)	1.8 (5.1)
	ZDP	2.8 (7.9)	1.8 (5.1)	1.5 (4.2)	**14.1 [2.8]**	1.9 (5.4)
	RAP	0.4 (1.1)	3.9 (11.0)	2.2 (6.2)	1.0 (2.8)	**11.3 [2.5]**

c. *Pattern persistence and sequences*

Table 2 shows the pattern sequence between two consecutive days. The persistence is large and corresponds to 64.7% of the days. The high values of persistence of atmospheric patterns between two consecutive days indicate that the characteristic time for moving the different elements that configure each cluster is longer than a day. The most common daily sequences of patterns are the persistence of ZDP and LAB with 14.1% and 13.8%, respectively. This is not surprising since they are the two most common patterns in the region. Nonetheless, persistence is longer in LWS and LAB, in which the mean number of consecutive persisting days is 3.2 and 3.1 respectively. RAP shows the smallest value of both frequency of persistence (11.3%) and mean number of consecutive days (2.5 days).

Nonpersistence sequences correspond to 35.3% of the days, with each individual sequence below 4%. The most common sequences are the change from RAP to LAB, from LWS to RAP, and from LAB to ZDP. It is not surprising that the LWS to RAP (3.1%) and RAP to LAB (3.9%) sequences, along with LAB to LDP (2.7%) and LDP to LWS (2.6%), are so common. These four sequences (LWS → RAP → LAB → LDP → LWS) constitute a chain in which the synoptic waves move forward a quarter wavelength. In fact, the opposite sequences are in general very uncommon since they imply an anomalous westward motion of the synoptic waves. Not surprisingly, there are no sequences between LWS and LAB and vice versa, since that would imply a complete inversion of the ridges and lows in a day.

The LAB to ZDP (3.1%) sequence is also a common transition that occurs when the low over the Bellingshausen Sea moves southeastward and crosses the Antarctic Peninsula. After this situation, the change from ZDP to LWS (2.8%) is also common, probably due to the orographic cyclogenesis leeside of the Antarctic Peninsula (Mayes 1985). This chain (LAB → ZDP → LWS) may replace the chain of LAB → LDP → LWS when the flow is mainly zonal over the Drake Passage and explains why the transition from RAP to LAB has a larger frequency than the others. The complete cycle with these two chains is outlined in Fig. 4, and it is found that this cycle is reinforced in spring and autumn when the circulation at high latitudes is enhanced by the SAO, whereas it weakens in summer and winter (not shown). The fact that all clusters are implicated in one or both transition chains may explain the similar frequencies of all circulation patterns.

d. *Climate variability and linear trends*

Correlations between the annual and seasonal occurrence of atmospheric patterns with the SAM and ENSO indices are shown in Table 3. The annual occurrence of most patterns significantly correlates with SAM, with only the exception of RAP showing a weak correlation (p value < 0.1). Seasonal occurrences of patterns also show significant correlations with SAM with the exception of correlations with RAP in autumn, winter, and spring, and with LWS in summer. A positive SAM increases the occurrence of ZDP and

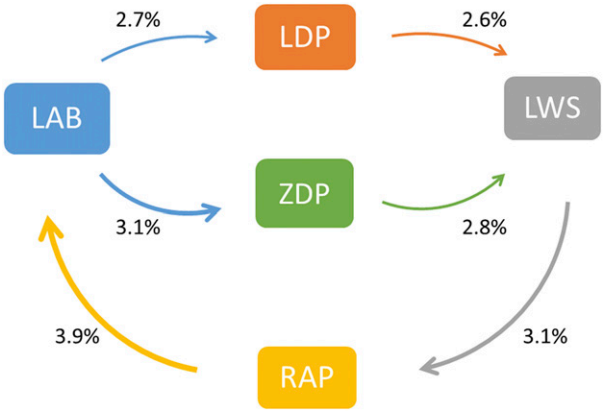

FIG. 4. Scheme of the most common transitions between synoptic patterns in the AP. The width of the arrows is proportional to the frequency of each transition.

TABLE 3. Correlations and statistical significance between the seasonal occurrence of synoptic patterns and SAM and El Niño–3.4 indices during the period between 1979 and 2016; p values are indicated in parentheses. Bolded values indicate statistically significant correlations at 95% confidence, and values in italics indicate statistically significant correlations at 90% confidence.

	Annual	DJF	MAM	JJA	SON
			SAM		
LWS	**−0.44 (0.006)**	−0.07 (0.674)	**−0.62 (0.000)**	**−0.39 (0.010)**	**−0.45 (0.005)**
LAB	**0.56 (0.000)**	**0.32 (0.048)**	**0.57 (0.000)**	**0.57 (0.000)**	**0.54 (0.000)**
LDP	**−0.53 (0.001)**	**−0.67 (0.000)**	**−0.41 (0.010)**	**−0.37 (0.020)**	**−0.71 (0.000)**
ZDP	**0.49 (0.002)**	**0.80 (0.000)**	**0.64 (0.000)**	**0.37 (0.023)**	**0.42 (0.008)**
RAP	−0.28 (0.094)	**−0.40 (0.011)**	−0.15 (0.379)	−0.10 (0.538)	*−0.29 (0.080)*
			El Niño–3.4		
LWS	**0.38 (0.017)**	*0.30 (0.062)*	0.16 (0.350)	**0.33 (0.043)**	**0.61 (0.000)**
LAB	**−0.39 (0.015)**	**−0.38 (0.018)**	**−0.34 (0.038)**	−0.22 (0.183)	**−0.52 (0.001)**
LDP	0.12 (0.452)	0.19 (0.257)	0.06 (0.738)	−0.14 (0.403)	0.20 (0.219)
ZDP	−0.20 (0.219)	−0.16 (0.322)	0.02 (0.908)	0.05 (0.789)	−0.01 (0.939)
RAP	0.01 (0.941)	−0.09 (0.579)	0.10 (0.559)	−0.12 (0.468)	−0.07 (0.684)

LAB since SAM is associated with the contraction and intensification of the circumpolar westerly belt that strengths zonal conditions (Lefebvre et al. 2004; Orr et al. 2008; Lubin et al. 2008), and it modulates the depth of the ABSL (Turner et al. 2013; Raphael et al. 2016; Clem and Fogt 2013). These two patterns contribute to bring mild air to the Antarctic Peninsula. By contrast, positive SAM reduces the occurrence of LDP and LWS. The SAM–LDP anticorrelation is consistent with other studies that show a reduction of the number of cyclones between 50° and 60°S due to the poleward shift of the polar jet and the cyclone path during positive SAM conditions (Reboita et al. 2015; Gallego et al. 2005), whereas the decrease of LWS occurrence with SAM may arise as a result of the zonal asymmetry of the SAM (Kidston et al. 2009; Fogt et al. 2012a), which is larger in winter than in summer (Codron 2005, 2007). Thus, the increase of the zonal symmetry in summer could explain the weak correlation between SAM and LWS in that season. Alternatively, RAP and SAM are weakly correlated for all seasons except summer. Hobbs and Raphael (2010) describe a climatological eastern Pacific anticyclone related to the zonal wave-3 (ZW3) pattern, the strength of which correlates with SAM in autumn and summer, when this high approaches the Drake Passage. We hypothesize that this relation may be behind the increase of the correlation between RAP and SAM in summer and to a lesser extent in autumn, although the relations with other climatological modes of variability may play a certain role complicating the interpretation.

Several studies have demonstrated that a tropospheric wave called the Pacific–South American (PSA) pattern strengthens and weakens the ABSL (Trenberth et al. 2002; Genthon and Cosme 2003). This pattern has been traditionally viewed as a response to the ENSO forcing, but recently Irving and Simmonds (2016) demonstrated a most complex nature of this pattern that is only partially modulated by ENSO and SAM. Nonetheless, a link between ENSO and ABSL has been determined, such that the cold (warm) phase of ENSO related to La Niña (El Niño) strengthens (weakens) the ABSL (Trenberth et al. 2002; Genthon and Cosme 2003), especially in spring when the correlations between ENSO and temperatures in the AP are strongest (Clem and Fogt 2013; Clem et al. 2016).

Our results show that ENSO has much lower influence in the atmospheric patterns over the AP region than SAM. Yet, there is a significant correlation between El Niño–3.4 SST anomalies and annual occurrences of LAB and LWS. These two patterns, unlike the other three, present centers of high and low pressure located almost in phase with the PSA. At a seasonal scale, El Niño–3.4 correlates with LAB in spring, summer, and autumn. Although investigations have shown that the correlation between ENSO and ABSL depth is greater in winter (Turner et al. 2013), the correlation between ENSO and LAB is weak, probably owing to the most western position of the low pressure center that goes outside of the regional limits. El Niño–3.4 also correlates with LWS in winter and spring, agreeing with the increase of the cyclonic density east to the AP during the positive phase of ENSO (Reboita et al. 2015, their Fig. 5).

It is worth noting that the correlations between ENSO or SAM and LAB occurrence are in agreement with the correlations between those teleconnections and the central pressure of ABSL calculated by Hosking et al. (2013, their Table 2). Both modes of variability affect the ABSL in a similar way, and it is known that these modes couple when they are in phase (Fogt and

TABLE 4. Annual and seasonal linear trends of synoptic pattern frequencies during the period between 1979 and 2016; p values are indicated in parentheses. Bolded values indicate statistically significant trends at 95% confidence, and values in italics indicate statistically significant correlations at 90% confidence.

	Annual	DJF	MAM	JJA	SON
LWS	−0.82 (0.329)	**2.72 (0.025)**	−2.43 (0.096)	−2.46 (0.114)	−0.42 (0.754)
LAB	**1.56 (0.047)**	0.40 (0.678)	**3.15 (0.009)**	−0.22 (0.868)	*3.10 (0.086)*
LDP	−0.79 (0.196)	−3.32 (0.065)	−0.24 (0.817)	1.18 (0.225)	0.09 (0.937)
ZDP	0.63 (0.409)	*3.11 (0.054)*	0.35 (0.778)	0.80 (0.431)	−1.33 (0.409)
RAP	−0.58 (0.210)	−1.20 (0.109)	−0.84 (0.470)	0.69 (0.557)	−1.16 (0.194)

Bromwich 2006; Fogt et al. 2011). Moreover, it is shown that ENSO and especially the SAM modulate the occurrence of the synoptic patterns over the AP. This synergy was also suggested by Pezza et al. 2012, who stated that large-scale stationary waves produced as a response of the different climate modes of variability may interact with transient eddies.

Related to stratospheric ozone depletion and greenhouse gas increases, SAM has shown a positive trend since 1958 (Thompson and Solomon 2002; Marshall et al. 2004), especially in summer and autumn. This increase in positive SAM conditions has contributed to an increase of the temperature in the AP during the last 60 years (Marshall 2007) by intensifying cyclonic conditions in high latitudes (Thompson and Solomon 2002), enhancing lee-side foehn winds on the eastern peninsula (Orr et al. 2008), and increasing meridional winds by amplifying the ABSL (Fogt et al. 2011, 2012b; Turner et al. 2013; Hosking et al. 2013). Therefore, it is expected to find a change in the patterns' occurrence associated with the increase of the SAM.

Table 4 shows the linear temporal evolution of frequency for each atmospheric pattern between 1979 and 2016. The only significant trends found at >95% significance are an increase of LWS in summer and an increase of LAB in autumn and all-year round. Weak trends are also observed in summer to increase ZDP and decrease LDP. The increase of LAB occurrences for both all-year round and autumn may be associated with the increase of SAM (Hosking et al. 2013; Raphael et al. 2016). The increase of zonal conditions in summer may enhance lee cyclogenesis around the Antarctic Peninsula (Mayes 1985; Orr et al. 2008), which would explain the increase of LWS occurrence in DJF.

4. Application to Livingston Island

The South Shetland Islands, as well as the northern edge of the Antarctic Peninsula, are located near the center of the study area. Thus, it is expected that the Livingston Ice Cap response may be influenced by the occurrence of the different circulation patterns advecting different air masses. This effect may be especially important in summer, when the ice caps are more sensitive to temperature changes. Indeed, Jonsell et al. (2012) have shown that the Livingston Ice Cap surface mass balance is very sensitive to small changes in temperature during the melt season, calculating that a 0.5°C increase results in 56% higher melt rates. They also noticed that high peaks in melt coincide with moist and warm fluxes arising from the northwest. This suggests that the LAB pattern may produce those peaks in melt.

Figure 5 shows the bivariate distribution of daily temperature and moisture anomalies with respect to the monthly mean for each circulation pattern at the JCI AWS on Livingston Island calculated using a kernel density estimation. As expected, LAB is prone to transporting warm and moist air to the Shetland Islands from the southeast Pacific whereas LWS and RAP advect cold and dry air from the continent. Therefore, those two patterns may largely affect the Livingston Ice Cap surface balance, being mainly negative during LAB conditions and stabilizing during LWS or RAP conditions. Both ZDP and LDP present mild temperatures, but whereas ZDP bears mainly moist air, LDP presents a dual behavior. LDP shows two peaks in the density function with different amounts of moisture. This behavior may be produced by different air advection depending on the position of the low with respect to the island. When the low is located west of Livingston, warm moist air is transported to JCI. When the low crosses to the east, the air becomes cooler and drier. Nonetheless, those relationships and their real effect on the cryosphere should be further explored.

Figure 6 shows the distribution of daily precipitation anomalies with respect to the monthly mean at the JCI AWS for each circulation pattern. Days with the LAB pattern present more positive precipitation anomalies. ZDP in general shows positive precipitation anomalies although it also presents many days with dry anomalies. Most of the dry days were classified as RAP, LWS, or LDP. It is worth noting that the dichotomy presented by LDP for moisture is also conspicuous for precipitation, with two relative peaks in the density function for both positive and negative precipitation

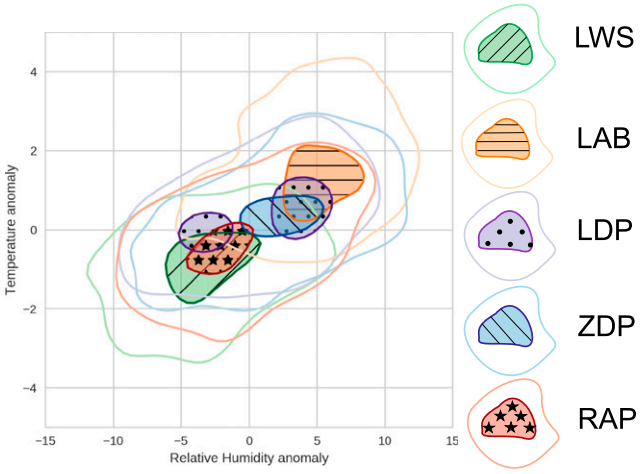

FIG. 5. Bivariate density function of daily temperature and relative humidity anomalies with respect to the monthly mean for each synoptic pattern at the JCI AWS. The period considered is between 2005 and 2016. Each pattern displays a different scale to better visualize the peak of the function (shaded).

anomalies. Indeed, the largest anomalies of precipitation at JCI (the right tail of the plot) are not produced by LAB but rather by the LDP and ZDP patterns. This indicates that LAB does not determine the largest precipitation episodes but rather light drizzle events. Those results should be carefully considered due to the limitations of the rain gauges when snowfall is collected.

5. Conclusions

Five synoptic pressure patterns have been computed from ERA-Interim reanalysis data using cluster analysis in the AP region (45°–75°S, 20°–120°W). The derived daily series of patterns from 1979 to 2016 is available to the scientific community through the AEMET public repository (http://hdl.handle.net/20.500.11765/7914). All five types present a similar frequency during the year, but they manifest a large seasonal variability as a result of changing climatological structures as the SAO, polar jet movement, etc. Transition between synoptic patterns tends to follow a cycle where synoptic waves move eastward a quarter wavelength. This cycle has two modes, one with a larger latitudinal amplitude and meridional circulation and another one with an enhanced zonal circulation. Indeed, climate modes of variability such as ENSO or SAM have a large influence in the frequency of patterns over the AP region. For example, as other studies suggest (e.g., Clem and Fogt 2013), the cold phase of ENSO in spring is associated with an enhanced ABSL and a reduction of the Weddell low. All synoptic patterns show a larger correlation with SAM than with ENSO. During the positive SAM, the ABSL becomes strengthened and zonal circulation increases. By contrast, lows over the Drake Passage and Weddell Sea prevail during the negative SAM. Indeed, the increase of LAB conditions may be explained by the increase of SAM as a result of stratospheric ozone depletion and greenhouse gas increases (Thompson and Solomon 2002; Marshall et al. 2004).

As pointed out by Cohen et al. (2013), there exist many potential uses for the synoptic patterns. In this paper, we conducted a cursory analysis to explore the

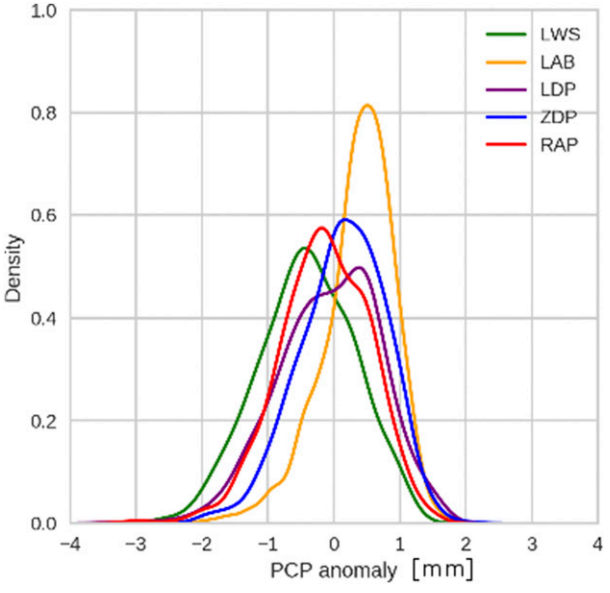

FIG. 6. Density function of daily precipitation anomalies with respect to the monthly mean for each synoptic pattern at the JCI AWS. The period considered is between 2005 and 2016.

possibility of determining the airmass characteristics associated with each pattern that may affect the surface mass balance of the ice cap on Livingston Island. Synoptic patterns have been shown to be a useful tool to study airmass advections that may affect the surface mass balance of ice caps and ice sheets in the periphery of Antarctica. Different patterns may carry different air masses. For example, LAB transports a warm and moist air mass and often slight precipitation to the South Shetland Islands whereas LWS is associated with dry and cold air. We suggest that changes of synoptic type occurrences, especially in summer, may dramatically affect the stability of glaciers and island ice caps. Future work will further explore the effects on the cryosphere with changing synoptic types.

Acknowledgments. This work is supported by the Ministry of Economy and Competitiveness (MINECO) through the AEMET Antarctic program and by the Spanish Investigation Agency (AEI) and the European Regional Development Fund (FEDER), Grant CTM2016-79741-R for MICROAIRPOLAR project (to S. Gonzalez and F. Vasallo). Integrated Data Viewer (IDV) software from UCAR/Unidata was used in the analysis and visualization of the data. We also thank the two anonymous reviewers whose feedback helped to greatly improve this text. Finally, we want also thank all those meteorologists from the AEMET Antarctic Group who, during 30 years, have maintained the observations of the Juan Carlos I meteorological station; some of these data are used in this paper.

REFERENCES

Arthur, D., and S. Vassilvitskii, 2007: k-means++: The advantages of careful seeding. *Proc. 18th Annual ACM-SIAM Symp. on Discrete Algorithms*, Philadelphia, PA, Society for Industrial and Applied Mathematics, 1027–1035, ilpubs.stanford.edu/778/1/2006-13.pdf.

Bamston, A. G., M. Chelliah, and S. B. Goldenberg, 1997: Documentation of a highly ENSO-related SST region in the equatorial Pacific: Research note. *Atmos.–Ocean*, **35**, 367–383, https://doi.org/10.1080/07055900.1997.9649597.

Bañon, M., and F. Vasallo, 2015: AEMET en la Antártida: Climatología y meteorología sinóptica en las estaciones meteorológicas en las estaciones meteorológicas españolas en la Antártida. AEMET, 150 pp.

Bliss, A., R. Hock, and J. G. Cogley, 2013: A new inventory of mountain glaciers and ice caps for the Antarctic periphery. *Ann. Glaciol.*, **54**, 191–199, https://doi.org/10.3189/2013AoG63A377.

Bracegirdle, T. J., and G. J. Marshall, 2012: The reliability of Antarctic tropospheric pressure and temperature in the latest global reanalyses. *J. Climate*, **25**, 7138–7146, https://doi.org/10.1175/JCLI-D-11-00685.1.

Carleton, A. M., 2003: Atmospheric teleconnections involving the Southern Ocean. *J. Geophys. Res.*, **108**, 8080, https://doi.org/10.1029/2000JC000379.

Carrasco, J. F., 2013: Decadal changes in the near-surface air temperature in the western side of the Antarctic Peninsula. *Atmos. Climate Sci.*, **3**, 275–281, https://doi.org/10.4236/acs.2013.33029.

Clem, K. R., and R. L. Fogt, 2013: Varying roles of ENSO and SAM on the Antarctic Peninsula climate in austral spring. *J. Geophys. Res. Atmos.*, **118**, 11 481–11 492, https://doi.org/10.1002/jgrd.50860.

——, J. A. Renwick, J. McGregor, and R. L. Fogt, 2016: The relative influence of ENSO and SAM on Antarctic Peninsula climate. *J. Geophys. Res. Atmos.*, **121**, 9324–9341, https://doi.org/10.1002/2016JD025305.

Codron, F., 2005: Relation between annular modes and the mean state: Southern Hemisphere summer. *J. Climate*, **18**, 320–330, https://doi.org/10.1175/JCLI-3255.1.

——, 2007: Relations between annular modes and the mean state: Southern Hemisphere winter. *J. Atmos. Sci.*, **64**, 3328–3339, https://doi.org/10.1175/JAS4012.1.

Cohen, L., S. Dean, and J. Renwick, 2013: Synoptic weather types for the Ross Sea region, Antarctica. *J. Climate*, **26**, 636–649, https://doi.org/10.1175/JCLI-D-11-00690.1.

Dee, D. P., and Coauthors, 2011: The ERA-Interim reanalysis: Configuration and performance of the data assimilation system. *Quart. J. Roy. Meteor. Soc.*, **137**, 553–597, https://doi.org/10.1002/qj.828.

Fogt, R. L., and D. H. Bromwich, 2006: Decadal variability of the ENSO teleconnection to the high-latitude South Pacific governed by coupling with the southern annular mode. *J. Climate*, **19**, 979–997, https://doi.org/10.1175/JCLI3671.1.

——, ——, and K. M. Hines, 2011: Understanding the SAM influence on the South Pacific ENSO teleconnection. *Climate Dyn.*, **36**, 1555–1576, https://doi.org/10.1007/s00382-010-0905-0.

——, J. M. Jones, and J. Renwick, 2012a: Seasonal zonal asymmetries in the southern annular mode and their impact on regional temperature anomalies. *J. Climate*, **25**, 6253–6270, https://doi.org/10.1175/JCLI-D-11-00474.1.

——, A. J. Wovrosh, R. A. Langen, and I. Simmonds, 2012b: The characteristic variability and connection to the underlying synoptic activity of the Amundsen-Bellingshausen Seas low. *J. Geophys. Res.*, **117**, D07111, https://doi.org/10.1029/2011JD017337.

Gallego, D., P. Ribera, R. Garcia-Herrera, E. Hernandez, and L. Gimeno, 2005: A new look for the Southern Hemisphere jet stream. *Climate Dyn.*, **24**, 607–621, https://doi.org/10.1007/s00382-005-0006-7.

Gardner, A. S., and Coauthors, 2013: A reconciled estimate of glacier contributions to sea level rise: 2003 to 2009. *Science*, **340**, 852–857, https://doi.org/10.1126/science.1234532.

Genthon, C., and E. Cosme, 2003: Intermittent signature of ENSO in west-Antarctic precipitation. *Geophys. Res. Lett.*, **30**, 2081, https://doi.org/10.1029/2003GL018280.

Govorukha, L. S., and V. Y. Timofeyev, 2002: Synoptic circulation types of Antarctic Peninsula and adjacent South Ocean regions and connected phenomena. *Probl. Klimatol. Polarn.*, **10**, 159–178.

Guijarro, J. A., 2017: Daily series homogenization and gridding with Climatol v.3. *Proc. Ninth Seminar for Homogenization and Quality Control in Climatological Databases and Fourth Conf. on Spatial Interpolation Techniques in Climatology and Meteorology*, Budapest, Hungary, EUMETNET, 175–182, www.climatol.eu/homClimatol3-a3.pdf.

Hobbs, W. R., and M. N. Raphael, 2010: Characterizing the zonally asymmetric component of the SH circulation. *Climate Dyn.*, **35**, 859–873, https://doi.org/10.1007/s00382-009-0663-z.

Hock, R., M. De Woul, V. Radić, and M. Dyurgerov, 2009: Mountain glaciers and ice caps around Antarctica make a

large sea-level rise contribution. *Geophys. Res. Lett.*, **36**, L07501, https://doi.org/10.1029/2008GL037020.

Hosking, J. S., A. Orr, G. J. Marshall, J. Turner, and T. Phillips, 2013: The influence of the Amundsen–Bellingshausen Seas low on the climate of West Antarctica and its representation in coupled climate model simulations. *J. Climate*, **26**, 6633–6648, https://doi.org/10.1175/JCLI-D-12-00813.1.

Houssos, E. E., C. J. Lolis, and A. Bartzokas, 2008: Atmospheric circulation patterns associated with extreme precipitation amounts in Greece. *Adv. Geosci.*, **17**, 5–11, https://doi.org/10.5194/adgeo-17-5-2008.

IPCC, 2013: *Climate Change 2013: The Physical Science Basis.* Cambridge University Press, 1535 pp.

Irving, D., and I. Simmonds, 2015: A novel approach to diagnosing Southern Hemisphere planetary wave activity and its influence on regional climate variability. *J. Climate*, **28**, 9041–9057, https://doi.org/10.1175/JCLI-D-15-0287.1.

——, and ——, 2016: A new method for identifying the Pacific–South American pattern and its influence on regional climate variability. *J. Climate*, **29**, 6109–6125, https://doi.org/10.1175/JCLI-D-15-0843.1.

Jonsell, U. Y., F. J. Navarro, M. Bañón, J. J. Lapazaran, and J. Otero, 2012: Sensitivity of a distributed temperature-radiation index melt model based on AWS observations and surface energy balance fluxes, Hurd Peninsula glaciers, Livingston Island, Antarctica. *Cryosphere*, **6**, 539–552, https://doi.org/10.5194/tc-6-539-2012.

Kejna, M., 1993: Types of atmospheric circulation in the region of H. Arctowski Station (South Shetland Islands) in the years 1986–1989. *Proc. XX Polar Symp.*, Lublin, Poland, Polish Academy of Sciences, 369–378.

Kidson, J. W., 2000: An analysis of New Zealand synoptic types and their use in defining weather regimes. *Int. J. Climatol.*, **20**, 299–316, https://doi.org/10.1002/(SICI)1097-0088(20000315)20:3<299::AID-JOC474>3.0.CO;2-B.

Kidston, J., J. A. Renwick, and J. McGregor, 2009: Hemispheric-scale seasonality of the southern annular mode and impacts on the climate of New Zealand. *J. Climate*, **22**, 4759–4770, https://doi.org/10.1175/2009JCLI2640.1.

Lana, A., J. Campins, A. Genovés, and A. Jansà, 2007: Atmospheric patterns for heavy rain events in the Balearic Islands. *Adv. Geosci.*, **12**, 27–32, https://doi.org/10.5194/adgeo-12-27-2007.

Lefebvre, W., H. Goosse, R. Timmermann, and T. Fichefet, 2004: Influence of the southern annular mode on the sea ice–ocean system. *J. Geophys. Res.*, **109**, C09005, https://doi.org/10.1029/2004JC002403.

Lubin, D., R. A. Wittenmyer, D. H. Bromwich, and G. J. Marshall, 2008: Antarctic Peninsula mesoscale cyclone variability and climatic impacts influenced by the SAM. *Geophys. Res. Lett.*, **35**, L02808, https://doi.org/10.1029/2007GL032170.

Ludescher, J., A. Bunde, C. L. E. Franzke, and H. J. Schellnhuber, 2016: Long-term persistence enhances uncertainty about anthropogenic warming of Antarctica. *Climate Dyn.*, **46**, 263–271, https://doi.org/10.1007/s00382-015-2582-5.

Marshall, G. J., 2003: Trends in the southern annular mode from observations and reanalyses. *J. Climate*, **16**, 4134–4143, https://doi.org/10.1175/1520-0442(2003)016<4134:TITSAM>2.0.CO;2.

——, 2007: Half-century seasonal relationships between the southern annular mode and Antarctic temperatures. *Int. J. Climatol.*, **27**, 373–383, https://doi.org/10.1002/joc.1407.

——, P. A. Stott, J. Turner, W. M. Connolley, J. C. King, and T. A. Lachlan-Cope, 2004: Causes of exceptional atmospheric circulation changes in the Southern Hemisphere. *Geophys. Res. Lett.*, **31**, L14205, https://doi.org/10.1029/2004GL019952.

——, A. Orr, N. P. M. van Lipzig, and J. C. King, 2006: The impact of a changing Southern Hemisphere annular mode on Antarctic Peninsula summer temperatures. *J. Climate*, **19**, 5388–5404, https://doi.org/10.1175/JCLI3844.1.

Mayes, P. R., 1985: Secular variations in cyclone frequencies near the Drake Passage, southwest Atlantic. *J. Geophys. Res.*, **90**, 5829–5839, https://doi.org/10.1029/JD090iD03p05829.

Oliva, M., F. Navarro, F. Hrbáček, A. Hernández, D. Nývlt, P. Pereira, J. Ruiz-Fernández, and R. Trigo, 2017: Recent regional climate cooling on the Antarctic Peninsula and associated impacts on the cryosphere. *Sci. Total Environ.*, **580**, 210–223, https://doi.org/10.1016/j.scitotenv.2016.12.030.

Orr, A., G. J. Marshall, J. C. R. Hunt, J. Sommeria, C.-G. Wang, N. P. M. van Lipzig, D. Cresswell, and J. C. King, 2008: Characteristics of summer airflow over the Antarctic Peninsula in response to recent strengthening of westerly circumpolar winds. *J. Atmos. Sci.*, **65**, 1396–1413, https://doi.org/10.1175/2007JAS2498.1.

Pezza, A. B., H. A. Rashid, and I. Simmonds, 2012: Climate links and recent extremes in Antarctic sea ice, high-latitude cyclones, southern annular mode and ENSO. *Climate Dyn.*, **38**, 57–73, https://doi.org/10.1007/s00382-011-1044-y.

Radić, V., and R. Hock, 2010: Regional and global volumes of glaciers derived from statistical upscaling of glacier inventory data. *J. Geophys. Res.*, **115**, F01010, https://doi.org/10.1029/2009JF001373.

——, and ——, 2011: Regionally differentiated contribution of mountain glaciers and ice caps to future sea-level rise. *Nat. Geosci.*, **4**, 91–94, https://doi.org/10.1038/ngeo1052.

Raphael, M. N., 2004: A zonal wave 3 index for the Southern Hemisphere. *Geophys. Res. Lett.*, **31**, L23212, https://doi.org/10.1029/2004GL020365.

——, and Coauthors, 2016: The Amundsen Sea low: Variability, change, and impact on Antarctic climate. *Bull. Amer. Meteor. Soc.*, **97**, 111–121, https://doi.org/10.1175/BAMS-D-14-00018.1.

Rayner, N. A., D. E. Parker, E. B. Horton, C. K. Folland, L. V. Alexander, D. P. Rowell, E. C. Kent, and A. Kaplan, 2003: Global analyses of sea surface temperature, sea ice, and night marine air temperature since the late nineteenth century. *J. Geophys. Res.*, **108**, 4407, https://doi.org/10.1029/2002JD002670.

Reboita, M. S., R. P. da Rocha, T. Ambrizzi, and C. D. Gouveia, 2015: Trend and teleconnection patterns in the climatology of extratropical cyclones over the Southern Hemisphere. *Climate Dyn.*, **45**, 1929–1944, https://doi.org/10.1007/s00382-014-2447-3.

Simmonds, I., and K. Keay, 2000: Mean Southern Hemisphere extratropical cyclone behavior in the 40-year NCEP–NCAR reanalysis. *J. Climate*, **13**, 873–885, https://doi.org/10.1175/1520-0442(2000)013<0873:MSHECB>2.0.CO;2.

——, and K. C. King, 2004: Global and hemispheric climate variations affecting the Southern Ocean. *Antarct. Sci.*, **16**, 401–413, https://doi.org/10.1017/S0954102004002226.

——, K. Keay, and E.-P. Lim, 2003: Synoptic activity in the seas around Antarctica. *Mon. Wea. Rev.*, **131**, 272–288, https://doi.org/10.1175/1520-0493(2003)131<0272:SAITSA>2.0.CO;2.

Thompson, D. W. J., and S. Solomon, 2002: Interpretation of recent Southern Hemisphere climate change. *Science*, **296**, 895–899, https://doi.org/10.1126/science.1069270.

Trenberth, K. E., J. M. Caron, D. P. Stepaniak, and S. Worley, 2002: Evolution of El Niño–Southern Oscillation and global atmospheric surface temperatures. *J. Geophys. Res.*, **107**, 4065, https://doi.org/10.1029/2000JD000298.

Turner, J., and Coauthors, 1996: The Antarctic First Regional Observing Study of the Troposphere (FROST) project. *Bull. Amer. Meteor. Soc.*, **77**, 2007–2032, https://doi.org/10.1175/1520-0477(1996)077<2007:TAFROS>2.0.CO;2.

——, G. J. Marshall, and T. A. Lachlan-Cope, 1998: Analysis of synoptic-scale low pressure systems within the Antarctic Peninsula sector of the circumpolar trough. *Int. J. Climatol.*, **18**, 253–280, https://doi.org/10.1002/(SICI)1097-0088(19980315)18:3<253::AID-JOC248>3.0.CO;2-3.

——, T. Phillips, J. S. Hosking, G. J. Marshall, and A. Orr, 2013: The Amundsen Sea low. *Int. J. Climatol.*, **33**, 1818–1829, https://doi.org/10.1002/joc.3558.

——, and Coauthors, 2016: Absence of 21st century warming on Antarctic Peninsula consistent with natural variability. *Nature*, **535**, 411–415, https://doi.org/10.1038/nature18645.

van den Broeke, M. R., 1998: The semi-annual oscillation and Antarctic climate. Part I: Influence on near surface temperatures (1957–79). *Antarct. Sci.*, **10**, 175–183, https://doi.org/10.1017/S0954102098000248.

——, 2000: The semi-annual oscillation and Antarctic climate. Part 3: The role of near-surface wind speed and cloudiness. *Int. J. Climatol.*, **20**, 117–130, https://doi.org/10.1002/(SICI)1097-0088(200002)20:2<117::AID-JOC481>3.0.CO;2-B.

——, and N. P. M. van Lipzig, 2003: Response of wintertime Antarctic temperatures to the Antarctic Oscillation: Results of a regional climate model. *Antarctic Peninsula Climate Variability: Historical and Paleoenvironmental Perspectives*, Antarctic Research Series, Vol. 79, Amer. Geophys. Union, 43–58.

van Loon, H., 1967: The half-yearly oscillations in middle and high southern latitudes and the coreless winter. *J. Atmos. Sci.*, **24**, 472–486, https://doi.org/10.1175/1520-0469(1967)024<0472:THYOIM>2.0.CO;2.

——, and R. L. Jenne, 1972: The zonal harmonic standing waves in the Southern Hemisphere. *J. Geophys. Res.*, **77**, 992–1003, https://doi.org/10.1029/JC077i006p00992.

Vaughan, D. G., and Coauthors, 2003: Recent rapid regional climate warming on the Antarctic Peninsula. *Climatic Change*, **60**, 243–274, https://doi.org/10.1023/A:1026021217991.